Enhanced indirect exchange interactions in the presence of circular potentials in graphene

Ahmet Utku Canbolat and Özgür Çakır

Physics Department, Izmir Institute of Technology, 35430, Urla, Izmir, Turkey

We calculate indirect exchange interaction between two magnetic impurities in pristine graphene in the presence of a circular potential. In bulk graphene structures indirect exchange interaction, also known as RKKY (Ruderman-Kittel-Kasuya-Yosida) interaction, shows a power-law decay with distance for both doped and undoped cases. Here we show that under a circular electric potential quasibound states lead to enhanced RKKY interactions between magnetic moments located in the vicinity of the potential well. It is shown that the strength of the potential well and Fermi energy can be tuned to create enhanced, nondecaying, long ranged RKKY interactions. We show that when the Fermi level lies at the quasibound state energy, the scattering processes between the states of the same chirality dominate over the other scattering channels and this leads to a predominantly ferromagnetic, nondecaying interaction between the impurities at long distances. The predicted effect can enable electrical control of RKKY interactions in graphene or other two-dimensional materials.

Graphene has been of intense theoretical and experimental interest due to its unusual electronic properties. Around Dirac points the conduction electrons can be effectively modeled by a massless Dirac equation, thus electrons behave as chiral particles different from ordinary metals [1]. Around Dirac points electrons exhibit Klein tunneling which makes it difficult to control electrons using external fields in pristine graphene [2]. However, it has been theoretically shown that it may still be possible to create quasibound states (QBS) using external electric fields [3–6]. Magnetic fields combined with electric fields were also shown to produce confinement in pristine graphene [7–10]. Scanning tunneling microscope (STM) measurements have shown the presence of quasibound states in circularly symmetric electrostatic potentials [11–15], where a STM tip enables the electrostatic confinement as well.

RKKY interaction [16–18] between magnetic impurities has been studied for graphene and bilayer graphene structures [19–23]. It has been found that in neutral graphene RKKY interaction has ferromagnetic character for magnetic moments located at the same sublattice, and antiferromagnetic for magnetic moments located at different sublattices. This behavior arises from the chiral nature of the electrons and the particle-hole symmetry in graphene [19]. In pristine graphene RKKY interaction decays with distance in the form $1/R^3$. On doping this behavior is modified, magnetic interaction switches between ferromagnetic and antiferromagnetic character at a period of Fermi wavelength as a function of distance and at large distances the RKKY interactions feature a $1/R^2$ type power-law decay [24–26]. Power *et al.* [27] reported an exchange energy decaying as $1/R$ at long distances when magnetic moments are driven by a time dependent magnetic field.

RKKY interaction in bilayer graphene with Bernal stacking was studied by Jiang *et al.* [28] and Klier *et al.* [29]. Due to change in energy dispersion and nonvanishing DOS, as well as the broken symmetry of the graphene layer, sublattices Jiang *et al.* predicted changes in exponents of power-law decays,

$1/R^n$, $n = 2, 3, 4, 6$, depending on sublattice type and layer indices of the magnetic moments [28]. Klier *et al.* predicted different regimes of RKKY interaction with changing Fermi energy in bilayer graphene. They have shown that when Fermi energy approaches the gap edge from below/above the gap edge, they predicted a finite/diverging oscillation period in space, with a power-law decay $1/R^{5/2}$ at the gap edge [29]. They also reported that in bilayer graphene by applying an external field the ferromagnetic/antiferromagnetic character of RKKY interaction can be controlled [30]. Krainov *et al.* predicted an enhancement in RKKY interactions when the bound state energy of adatoms overlaps with the energy of occupied states of graphene [31].

Engineering electromagnetic density of states through optical cavities has led to a range of physical phenomena such as Purcell enhancement of spontaneous emission, coherent control of emitters, and Dicke superradiance in cavity QED systems [32]. Motivated by cavity QED systems we have investigated the possibility of creating electronic cavities and using the cavity modes to create enhanced, long ranged RKKY type magnetic interactions in graphene. The system we consider is shown in Fig. 1 where a circular potential well is introduced on bulk graphene and two magnetic moments are located inside this region. In the first part of this work the QBS and the LDOS are determined in the presence of a circular potential well, which are then used to calculate RKKY interactions.

Electrons around K, K' points in the Brillouin zone of graphene lattice, as shown in Fig. 1, behave as massless Dirac fermions [1,33]. The Hamiltonians around the two Dirac points are given as

$$H_K = V(\mathbf{r})\sigma_0 + v_F \, \boldsymbol{\sigma} \cdot \mathbf{p},$$
$$H_{K'} = V(\mathbf{r})\sigma_0 + v_F \, \boldsymbol{\sigma}^* \cdot \mathbf{p}. \quad (1)$$

Here $\mathbf{p} = p_x \hat{e}_x + p_y \hat{e}_y$ is the momentum of the electron in the two-dimensional graphene sheet. $V = V(\mathbf{r})$ is the
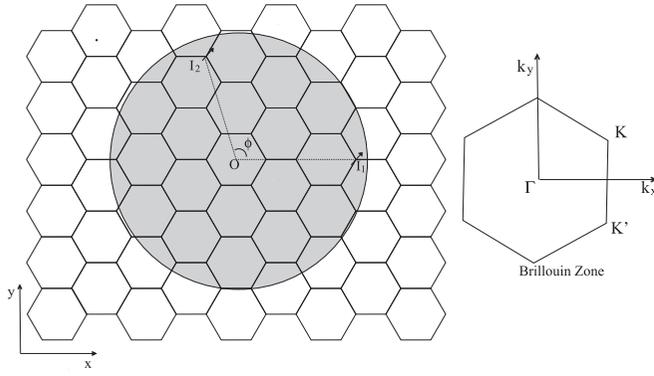
FIG. 1. In a circular region of graphene an attractive potential $-V_0$ is introduced where two magnetic moments are placed inside the potential well region as shown in the left panel. The Brillouin region for graphene lattice is shown in the right panel, where K, K' are the Dirac points.

potential energy function, $(\sigma_0)_{ij} = \delta_{ij}$ and $\{\sigma_\alpha, \alpha = x, y, z\}$ are the Pauli matrices, and $v_F \simeq 1.0 \times 10^6$ m/s is the Fermi velocity of electrons around Dirac points. Around K Dirac point $J_z = L_z + \hbar\sigma_z/2$ is the total angular momentum operator, with orbital angular momentum operator $L_z = xp_y - yp_x$, and the pseudospin operator $\hbar\hat{\sigma}/2$. Around Dirac point K', the total angular momentum operator is given as $J_z = L_z - \hbar\sigma_z/2$.

We will consider an attractive circular well potential

$$V(r) = -V_0\theta(R - r), \tag{2}$$

where $\theta(x)$ is the Heaviside step function. For the circular potential Eq. (2), the eigenstates of $H_{K(K')}$ [Eq. (1)] of energy E, and the total angular momentum quantum number $j = m \pm 1/2$ around $K(K')$ Dirac points, are given as follows [4–6]:

$$\psi_m^{K(K')}(k, r) = \begin{cases} \frac{A}{\sqrt{4\pi}} \left(\begin{smallmatrix} J_m(qr) \\ \pm is_1 J_{m\pm1}(qr)e^{\pm i\varphi} \end{smallmatrix} \right) e^{im\varphi}, & r < R, \\ \frac{\cos\theta}{\sqrt{4\pi}} \left(\begin{smallmatrix} J_m(kr) \\ \pm is_2 J_{m\pm1}(kr)e^{\pm i\varphi} \end{smallmatrix} \right) e^{im\varphi} - \frac{\sin\theta}{\sqrt{4\pi}} \left(\begin{smallmatrix} N_m(kr) \\ \pm is_2 N_{m\pm1}(kr)e^{\pm i\varphi} \end{smallmatrix} \right) e^{im\varphi}, & r > R, \end{cases}$$

$$k = \frac{E}{s_2 \hbar v_F}, \quad q = \frac{E + V_0}{s_1 \hbar v_F}, \tag{3}$$

corresponding to energy $E = -V_0 + s_1 \hbar v_F q = s_2 \hbar v_F k$, with the phase shift θ, where m is an integer. Depending on the energy $s_1 = \text{sgn}(E + V_0)$, $s_2 = \text{sgn}(E)$. Imposing the continuity of the wave function at the potential well boundary $r = R$, A and θ are obtained as follows:

$$A = \frac{2s_1 s_2}{\pi kR} \frac{1}{\sqrt{f_m^2 + g_m^2}}, \quad \tan\theta = \frac{f_m}{g_m}, \tag{4}$$

$$f_m(E) = J_m(qR)J_{m\pm1}(kR) - s_1 s_2 J_{m\pm1}(qR)J_m(kR),$$

$$g_m(E) = J_m(qR)N_{m\pm1}(kR) - s_1 s_2 J_{m\pm1}(qR)N_m(kR). \tag{5}$$

In Fig. 2(a) the $\text{DOS}(r < R) = \int_{r<R} d^2\mathbf{r} \text{LDOS}(r)$ which is the LDOS integrated within the potential well region is shown as a function of strength of the potential $|V|$ and the momentum of the electron within the potential well region q. Resonances appear at energies close to $E = 0(q = V/\hbar v_F)$. At $E = 0$ LDOS vanishes everywhere since this energy value corresponds to the Dirac point outside the potential well region and resonances appear [34] which are attained for $\theta = \pi/2 \to g_m(E) = 0$, whereas the width of resonances are determined by the function $f_m(E)$ [13]. In Fig. 2(b) the LDOS in the potential well region is shown for $V_0 = 4\hbar v_F/R$. It is seen that the sharpest resonance is due to $j = 1/2$ state, whereas with increasing angular momentum values the amplitudes of resonances decrease [4,6,35].

In Fig. 3 the width of $\text{DOS}(r<R)$ and its value at the QBS values is shown for $VR/\hbar v_F = 4, 8, 12$. With increasing potential energy QBS become sharper and they are attained at higher angular momentum values.

We are going to consider two magnetic moments located at (r_i, ϕ_i), $i = 1, 2$ both inside the potential well region $r_{1(2)} < R$. The magnetic moments interact with the electrons

in the π_z orbitals of the graphene, through an on-site exchange interaction

$$V = \sum_{n=1,2} J_n \mathbf{I_n} \cdot \mathbf{S} \delta(\mathbf{r} - \mathbf{r}_n), \tag{6}$$

with spin $1/2$ magnetic impurities $\mathbf{I}_{1(2)}$, electron spin $\mathbf{S}$, coupling strength $J_{1(2)}$, and position $r_{1(2)}$. The effective exchange interaction between the magnetic moments can be written as follows:

$$V_{\text{RKKY}} = J_{\alpha\beta} \mathbf{I}_1 \cdot \mathbf{I}_2, \tag{7}$$

where $\alpha(\beta) = A, B$ denotes the sublattice type for the impurities. For graphene there arises two cases where both impurities interact with the atoms in the same sublattice in which case RKKY interaction is denoted by $J_{AA(BB)}$ or impurities may be located at a different sublattice with RKKY interaction given by $J_{AB(BA)}$. The exchange interaction constant can be computed through spin susceptibility [21]

$$J_{\alpha\beta}(\mathbf{r}, \mathbf{r}') = -\frac{J_1 J_2}{2\pi} \int^{E_F} dE \, \text{Im}\big[G_{\alpha\beta}^0(\mathbf{r}, \mathbf{r}')G_{\beta\alpha}^0(\mathbf{r}', \mathbf{r})\big], \tag{8}$$

where the noninteracting Green function is given as $G^0(\mathbf{r}, \mathbf{r}', E) = \langle\mathbf{r}|(E - H_0 + i\delta)^{-1}|\mathbf{r}'\rangle$. Using the eigenfunctions (3) RKKY interaction can be expressed as follows:

$$J_{\alpha\beta}(\mathbf{r}, \mathbf{r}') = 2J_1 J_2 \sum_{m,m',\tau,\tau'} \int_0^\infty kdk \int_0^\infty k'dk'$$

$$\times \frac{\psi_{m\alpha}^{\tau *}(k, \mathbf{r}')\psi_{m'\alpha}^{\tau'}(k', \mathbf{r}')\psi_{m'\beta}^{\tau' *}(k', \mathbf{r})\psi_{m\beta}^\tau(k, \mathbf{r})}{E_k - E_{k'}}$$

$$\times n_k(1 - n_k'), \tag{9}$$
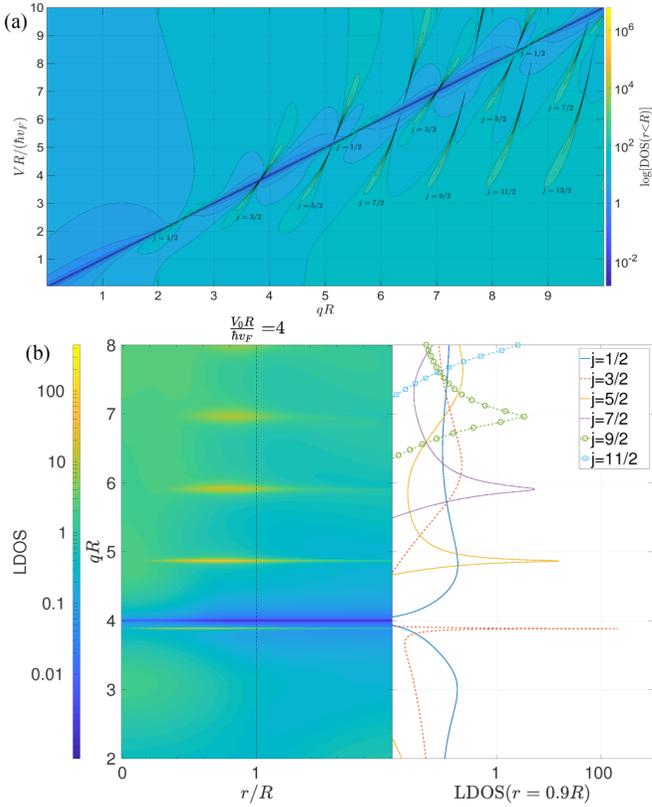
FIG. 2. (a) DOS($r < R$) is shown as a function of strength of the potential well V and radial momentum $q = (E + V_0)/\hbar v_F$, where R is the radius of the quantum well. The $\hbar v_F q = V$ line (deep blue line) corresponds to the charge neutral energy point at regions $r \gg R$, with a vanishing DOS and in the vicinity of this energy region quasibound states emerge. (b) LDOS for $V = 4\hbar v_F/R$ is shown in the left panel, as a function of radial momentum q and distance from the center of the potential well r. Again at $\hbar v_F q = V$ the LDOS is seen to be depleted. $r \lessgtr R$ regions correspond to interior (exterior) parts of the quantum well region. With increasing angular momentum, QBSs become more localized at the quantum well boundary. In the right panel LDOS at $r = 0.9R$ is shown as a function of qR (leftmost vertical axis), for angular momentum values $j = 1/2, 3/2, \ldots, 11/2$.

where τ, τ' are the valley indices, and α, β are the sublattice types of the impurities. The result (9) describes a second order scattering process which gives rise to an effective coupling between two magnetic moments [36].

We are going to consider the case when two impurities are located inside the potential well region at distances r_1 and r_2 from the center of the potential well as shown in Fig. 1. First we will investigate the case when the position of the first impurity I_1 is fixed and position of the second impurity I_2 varies at fixed r_2 with angular position $0 < \phi < \pi$. The behavior of J_{AA} as a function of distance is shown for two magnetic impurities both located at a distance $r = 0.9R$ from the center of the quantum well in Figs. 4(a) and 4(b) at the quasibound state energies for angular momentum quantum number $j = 1/2$, $j = 3/2$, respectively. The fast oscillations at the scale of lattice constant are due to intervalley scattering, where the dashed line in Figs. 4(a) and 4(b) is the RKKY interaction averaged over atomic scale oscillations. These
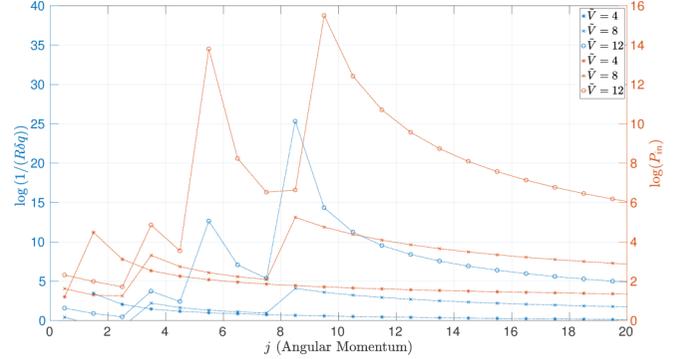
FIG. 3. The width of the DOS($r < R$) (blue curve) and its value (red curve) at the QBS energy is shown: $\tilde{V} = VR/\hbar v_F = 4, 8, 12$. In particular $j = 1/2$ state has no QBS for $\tilde{V} = 4$.

averaged values feature the spatial behavior of QBS states. It is seen that RKKY interaction is revived around the circular potential well region in contrast with the neutral/doped graphene, where a a power-law decay is predicted [25,26]. As the radius of the quantum well R increases, the strength of the RKKY interaction is suppressed with increasing radius of the potential well as $1/R^3$.

In neutral graphene, for impurities located at different sublattices, RKKY interaction is of antiferromagnetic character [19]. However, in the presence of an external potential at the quasibound energy, RKKY interaction switches to ferromagnetic behavior after some particular distance as shown in Figs. 4(c) and 4(d). In neutral graphene scattering between different Dirac cones leads to an antiferromagnetic behavior $J_{AB} > 0$. However, when the Fermi energy is at the quasibound state, energy scattering within the same Dirac cone dominates RKKY interaction and this leads to a ferromagnetic behavior. In Figs. 4(c) and 4(d) J_{AB} is averaged over oscillations at the lattice constant scale, and the eigenmode due to the potential well emerges (dashed line).

We have discussed the cases when the impurities are equidistant from the center of the potential well. Another case of interest is the case when the impurities are located at different distances from the center of the potential well. In Fig. 5(a) the case when impurities are located at $r_1 = 0.5R$ and $r_2 = 0.9R$ (solid curve) is compared with the case when the impurities are at equal distance from the center of the well at $r = 0.9R$ (dashed curve). No significant change is seen in the magnitude of J_{AA}. J_{AB} is shown in Fig. 5(b), where interestingly the ferromagnetic character dominates (solid curve) compared with the impurities located at the same distance from the center of the potential well (dashed curve).

Finally, we will discuss the case when the Fermi energy is not exactly at the quasibound state energy. In this case the quasibound state energy may lie below or above the Fermi energy, leading to enhanced scattering rate either for electron or hole states. In Fig. 6(b) the results for J_{AA} are shown for three cases $q_F = 3.8875/R$ which is the quasibound state energy and $q_F = 3.95/R$, $3.80/R$. It is seen that exchange interactions are suppressed in comparison with the case when Fermi is at the quasibound state energy. However, an enhancement at an order of magnitude is predicted in comparison with neutral graphene and very similar results are obtained for J_{AB} as well.
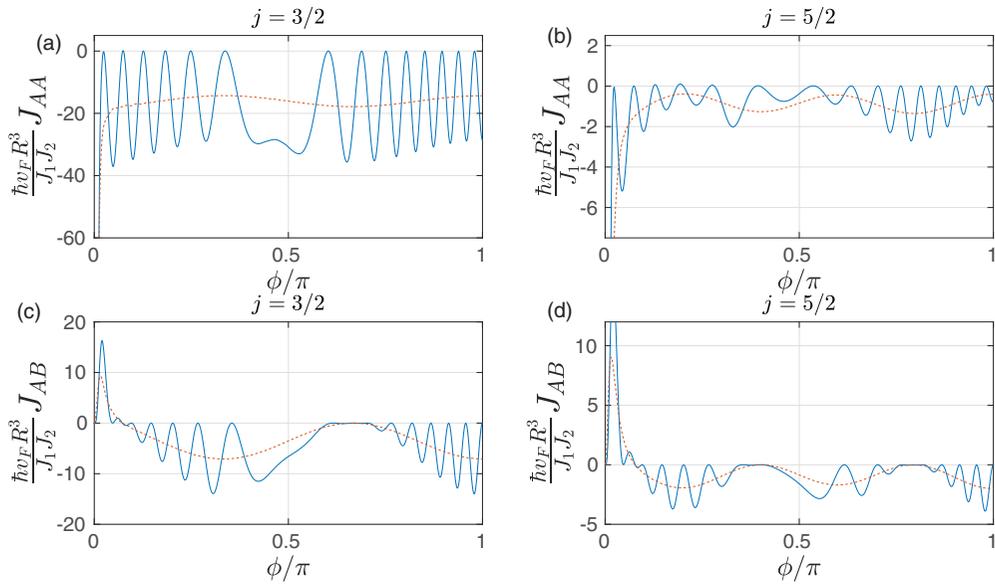
FIG. 4. RKKY interaction (solid) and its value averaged over oscillations at the atomic scale (dashed) where the Fermi level is at the the QBS energies for $V = 4\hbar v_F/R$, $R = 20a$: J_{AA} for (a) $q_F = 3.8875/R(j = 3/2)$, (b) $q_F = 4.8675/R(\ j = 5/2)$, and J_{AB} for (c) $q_F = 3.8875/R(j = 3/2)$, (d) $q_F = 4.8675/R(j = 5/2)$. Here R is the radius of the potential well.

However, compared to the case when Fermi energy is at the QBS energy, here the RKKY interaction oscillates between ferromagnetic and antiferromagnetic behavior for both J_{AA} and J_{AB}.

As a summary we have studied RKKY interactions in the presence of a circular potential in graphene nanostructures.

The QBS lead to an enhancement in LDOS in the vicinity of the potential well region. When the Fermi energy lies at/near one of these quasibound state energies, magnetic moments can interact strongly with each other via the Fermi sea electrons at
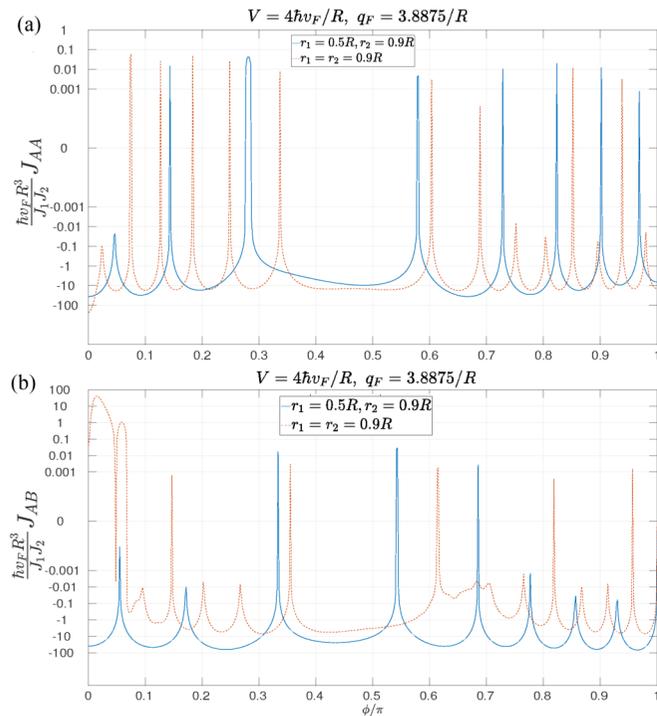
FIG. 5. (a) J_{AA} and (b) J_{AB} are shown for impurities located at $r_1 = 0.5R$, $r_2 = 0.9R$ (solid curve), and $r_1 = r_2 = 0.9R$ (dashed curve) where the Fermi level is at the quasibound state energy for $j = 3/2$ at $q_F = 3.8875/R$.
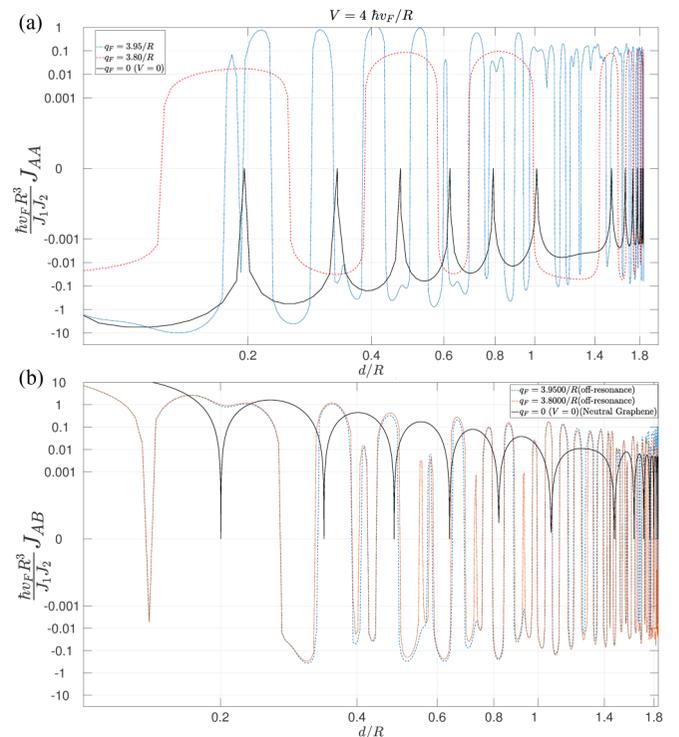
FIG. 6. (a) J_{AA} and (b) J_{AB} are shown for the case when both impurities are at the same distance from the center of the potential well, at varying relative angular positions along the periphery of the potential well, at $r = 0.9R$, for Fermi energy at $q_F = 3.95/R$ (dotted), $q_F = 3.80/R$ (dashed), and neutral graphene (solid). The horizontal axis is the distance between the impurities.

the quasibound state energy. When the Fermi energy is at the QBS energy, instead of a power-law decay which is typical for metals, numerically an enhanced RKKY interaction is predicted for impurity moments located in the vicinity of the circular potential well region. As the radius of the potential well region R increases, the strength of RKKY interaction is suppressed with $1/R^3$. However due to an enhanced LDOS at QBS energies, the RKKY interaction will be enhanced and exhibit revivals in the potential well region. RKKY interactions in neutral graphene can be of antiferromagnetic or ferromagnetic character depending on the sublattice type of impurity sites. However, in the presence of a circular well potential, beyond a certain distance, a ferromagnetic interaction dominates irrespective of the sublattice type of impurity sites.

The observed effects are not sensitive to the location of the impurity moments as long as they are in the vicinity of the potential well region.

Similar to external potentials, impurities, dislocations, or edge states may lead to enhancement of LDOS, which may lead to enhancement in RKKY interactions within the range of those localized states.

[1] A. H. Castro Neto, N. M. R. Peres, K. S. Novoselov, A. K. Geim, F. Guinea, and A. Neto, Rev. Mod. Phys. **81**, 109 (2009).

[2] A. F. Young and P. Kim, Nat. Phys. **5**, 222 (2009).

[3] J. M. Pereira, V. Mlinar, F. M. Peeters, and P. Vasilopoulos, Phys. Rev. B **74**, 045424 (2006).

[4] A. Matulis and F. M. Peeters, Phys. Rev. B **77**, 115423 (2008).

[5] J. H. Bardarson, M. Titov, and P. W. Brouwer, Phys. Rev. Lett. **102**, 226803 (2009).

[6] H. Chau Nguyen, N. T. T. Nguyen, and V. Lien Nguyen, J. Phys.: Condens. Matter **29**, 405301 (2017).

[7] A. De Martino, L. Dell'Anna, and R. Egger, Phys. Rev. Lett. **98**, 066802 (2007).

[8] H.-Y. Chen, V. Apalkov, and T. Chakraborty, Phys. Rev. Lett. **98**, 186803 (2007).

[9] A. V. Shytov, M. S. Rudner, and L. S. Levitov, Phys. Rev. Lett. **101**, 156804 (2008).

[10] G. Giavaras, P. A. Maksym, and M. Roy, J. Phys.: Condens. Matter **21**, 102201 (2009).

[11] Y. Zhao, J. Wyrick, F. D. Natterer, J. F. Rodriguez-Nieva, C. Lewandowski, K. Watanabe, T. Taniguchi, L. S. Levitov, N. B. Zhitenev, and J. A. Stroscio, Science **348**, 672 (2015).

[12] N. M. Freitag, L. A. Chizhova, P. Nemes-Incze, C. R. Woods, R. V. Gorbachev, Y. Cao, A. K. Geim, K. S. Novoselov, J. Burgdörfer, F. Libisch, and M. Morgenstern, Nano Lett. **16**, 5798 (2016).

[13] C. Gutiérrez, L. Brown, C.-J. Kim, J. Park, and A. N. Pasupathy, Nat. Phys. **12**, 1069 (2016).

[14] J. Lee, D. Wong, J. Velasco, Jr., J. F. Rodriguez-Nieva, S. Kahn, H.-Z. Tsai, T. Taniguchi, K. Watanabe, A. Zettl, F. Wang, L. S. Levitov, and M. F. Crommie, Nat. Phys. **12**, 1032 (2016).

[15] Y. Jiang, J. Mao, D. Moldovan, M. R. Masir, G. Li, K. Watanabe, T. Taniguchi, F. M. Peeters, and E. Y. Andrei, Nat. Nanotechnol. **12**, 1045 (2017).

[16] M. A. Ruderman and C. Kittel, Phys. Rev. **96**, 99 (1954).

[17] T. Kasuya, Prog. Theor. Phys. **16**, 45 (1956).

[18] K. Yosida, Phys. Rev. **106**, 893 (1957).

[19] S. Saremi, Phys. Rev. B **76**, 184430 (2007).

[20] E. H. Hwang and S. Das Sarma, Phys. Rev. Lett. **101**, 156802 (2008).

[21] M. Sherafati and S. Satpathy, Phys. Rev. B **83**, 165425 (2011).

[22] E. Kogan, Phys. Rev. B **84**, 115119 (2011).

[23] A. D. Güçlü and N. Bulut, Phys. Rev. B **91**, 125403 (2015).

[24] H. Sevincli, R. T. Senger, E. Durgun, and S. Ciraci, J. Phys.: Condens. Matter **19**, 216205 (2007).

[25] M. Sherafati and S. Satpathy, Phys. Rev. B **84**, 125416 (2011).

[26] E. Kogan, Graphene **02**, 8 (2013).

[27] S. R. Power, F. S. M. Guimarães, A. T. Costa, R. B. Muniz, and M. S. Ferreira, Phys. Rev. B **85**, 195411 (2012).

[28] L. Jiang, X. Lü, W. Gao, G. Yu, Z. Liu, and Y. Zheng, J. Phys.: Condens. Matter **24**, 206003 (2012).

[29] N. Klier, S. Shallcross, and O. Pankratov, Phys. Rev. B **90**, 245118 (2014).

[30] N. Klier, S. Sharma, O. Pankratov, and S. Shallcross, Phys. Rev. B **94**, 205436 (2016).

[31] I. V. Krainov, I. V. Rozhansky, N. S. Averkiev, and E. Lähderanta, Phys. Rev. B **92**, 155432 (2015).

[32] M. O. Scully and M. S. Zubairy, *Quantum Optics* (Cambridge University Press, Cambridge, 1997).

[33] G. W. Semenoff, Phys. Rev. Lett. **53**, 2449 (1984).

[34] P. E. Allain and J. N. Fuchs, Eur. Phys. J. B **83**, 301 (2011).

[35] R. L. Heinisch, F. X. Bronold, and H. Fehske, Phys. Rev. B **87**, 155409 (2013).

[36] C. Kittel, *Quantum Theory of Solids* (Wiley, New York, 1963).